Fluorescence Polarization Measurements of the Local Viscosity of Hydroxypropyl Guar in Solution

Trevor A. Smith,* Lisa M. Bajada, and David E. Dunstan†

School of Chemistry and CRC for Bioproducts, Department of Chemical Engineering, University of Melbourne, Victoria, 3010, Australia

Received June 1, 2001; Revised Manuscript Received November 25, 2001

ABSTRACT: The local viscosity experienced by the chain backbone of fluorescein-labeled hydroxypropylguar (HPG) in aqueous solution has been studied using time-resolved and steady-state fluorescence polarization spectroscopy. These measurements have been undertaken over a range of HPG concentrations and in a series of glycerol/water solutions of varying Newtonian viscosity. The results indicate that despite the bulk viscosities varying over several orders of magnitude as a function of HPG concentration, the rotational dynamics of the fluorophore attached to the backbone are only measurably affected at concentrations of ∼10 wt %. Samples of the HPG at concentrations as high as 10 wt % therefore contain regions with viscosity similar to the aqueous phase as sensed by the probe molecule. Intermolecular interaction between the chains introduces a slow rotational mode at concentrations approaching 10 wt %. The rotational correlation time of the probe attached to the HPG backbone shows a square root dependence on the solvent viscosity in the glycerol/water mixtures. This may be attributed to the restricted motion of the probe molecule around the central axis in two dimensions.

Introduction

The effects of polymer dynamics on the local and bulk rheological properties of polymers in solution are relevant to a range of physical phenomena. In particular, the complex flow behavior of concentrated polymer systems is influenced greatly by both intra- and intermolecular interactions of the polymer chains and also interactions between the polymer chain and the solvent.

The aims of this study were to determine the dynamics of polymer chains and quantify their interactions in solution for a biological polymer system—a derivatized form of guar gum. Guar is a naturally occurring galactomannan polysaccharide obtained from the endosperm of the legume *Cyamposis tetragonolobus* which is grown predominantly in arid and semiarid regions such as India and Pakistan.[1] The bulk viscosities of guar and its derivatives are able to be varied over several orders of magnitude (up to several Pa·s) as a function of modest polymer concentrations. The strong concentration/viscosity behavior exhibited leads to polysaccharides such as these having diverse applications in industry from food thickening agents to ink jet printers.[2] Despite their widespread commercial use, the dynamic behavior of polysaccharides in solution is an important area that is not fully understood. For example, it is not clear how the bulk viscosity behavior exhibited is influenced by the local viscosity and chain interactions.

Polymer systems exhibit a wide range of relaxation processes occurring over a broad range of time scales. It has been suggested that for dilute solutions the polymer backbone senses the solvent viscosity only,[3] and under these conditions the polymeric molecule as a whole has a characteristic rotational relaxation time on the order of 10^4-10^7 s^{-1}. For flexible molecules, small polymer chain segmental motions with rotational correlation times of the order $10^{-7}-10^{-9}$ s are also observed. Chromophores pendant to the chain can also rotate on the picosecond (and longer) time scales under these conditions. At higher polymer concentrations a critical value, c^*, is reached, which corresponds to the concentration of flexible polymer molecules at which the swollen polymer coils can no longer be accommodated without interpenetration. The critical overlap concentration, c^*, therefore separates the dilute from "semidilute" solutions, marking the characteristic changes in the concentration dependence of thermodynamic and hydrodynamic properties.[4,5] Under these conditions the time scales of motion of the chains and any pendant chromophores might be expected to begin to be altered relative to the dilute regime.

At concentrations exceeding the critical overlap concentration, the chains form a "solvent" (or melt) of comparatively small molecules. The polymer backbones sense the presence of the other polymer chains (N) and exhibit an effective local viscosity: $\eta_N = \eta_{mon}N^3$, where η_{mon} is the microscopic viscosity defined at the isolated monomer level.[3] The polymer solution behaves as a homogeneous solution with a characteristic mesh size or correlation length, ξ. Above c^*, the entangled macromolecules are restricted in their rotation, but segmental movement is relatively unaffected.[6] Oster and Nishijima[6] state that the local or microscopic viscosity is practically that of the solvent and rises only slowly with increasing polymer concentration. The local viscosity should reach a high value only for practically pure polymer where, because of the absence of solvent, the polymer segments are in direct contact and hence are severely restricted in their movements. The macroscopic viscosity, however, rises significantly with increasing polymer concentration above c^*. The time scales of the rotational motion of the macromolecule as a whole should thus be altered significantly whereas the time scales of segmental rotational motion, and that of any pendant chromophores, should not be affected to any large degree.

There are surprisingly few fluorescence-based experimental studies aimed at quantifying the polymer concentration dependence on the local viscosity experienced

† CRC for Bioproducts.
* Corresponding author. E-mail: trevoras@unimelb.edu.au.

10.1021/ma010954p CCC: $22.00
Published on Web 02/23/2002

by the chain backbone. The essential works may be summarized as follows. The earliest work of Biddle and Pardham used steady-state fluorescence polarization measurements with fluorescein attached to hydroxyethylcellulose.[7] These workers determined the frictional conditions experienced by the probe and quantified the activation energy associated with chain entanglement. Oster and Nishijima have also used steady-state fluorescence measurements to examine the local chain dynamics.[6] As mentioned above, these workers conclude that rotational segmental motion is relatively unaffected by entanglement with other polymer molecules. The later work of Hu et al. studied changes in the microenvironment of a fluorescent probe attached to PMMA during pH-induced volume phase transitions.[8] The viscosity dependence of the local segmental dynamics of synthetic polymers in dilute solution has been investigated by a number of workers. In particular, Ediger and co-workers have used time-resolved fluorescence anisotropy measurements (TRAMS) investigating anthracene-labeled polyisoprene as a function of viscosity and temperature.[9,10] Interestingly, as will be discussed later, these workers observed a $\tau \sim \eta^{0.75}$ relationship for a range of solvent conditions for their probe/polymer system. More recently, Soutar and Swanson[11] studied labeled poly(methacrylic acid) and found significant pH effects on the local probe motion in a manner similar to that observed by the Hu et al. group as referred to above.[8]

An attractive system for fluorescence studies of polymer chain dynamics is a polymer containing a covalently bound fluorophore which is held so as to form part of the polymer backbone. The systems most studied to date in this regard have employed anthracene as the midchain fluorescent probe in polymers of polyisoprene,[9,10,12] polystyrene,[13−16] polybutadiene,[17−19] and poly(methacrylic acid).[20] These elegant systems incorporate anthracene bound midchain through the 9,10 positions, thus restricting rotational motion to one degree; that being around the axis of the commonly photoexcited, short axis, transversly polarized ^1L_a absorption and emission transition dipoles. In this way the rotational motion of the probe should not contribute significantly to emission depolarization, and any such depolarization should reflect only the segmental ("crankshaft") motion of the chain. A similar approach was taken by Ushiki and Ozu,[21] who incorporated the proflavine fluorophore into the backbone of polyimides. Polymers with pendant fluorophores are also be capable of providing useful information and are often easier to synthesize than the midchain fluorophore counterparts, especially for biopolymer systems such as that studied here.

This work aims to investigate the dynamic rotational behavior of fluorescein pendant to the backbone of a hydroxypropyl-modified form of guar (HPG). This system has been examined over a range of solvent viscosities and as a function of polymer concentration far exceeding c^*. This has been done in order to assess the degree to which the probe senses the microenvironment (local viscosity) in which the chain resides. The results have been used to interpret the degree of molecular interactions between the chains and to correlate these with the macroscopic rheological behavior. A series of steady-state and time-resolved fluorescence anisotropy measurements have been conducted on five systems. First, solutions of free fluorescein in water/glycerol mixtures were studied as a reference for the experiments with HPG. The same measurements were carried out on a series of glycerol/water solutions containing free fluorescein with 0.5 wt % unlabeled HPG added. Third, measurements from glycerol/water solutions of a small amount of the fluorescein-labeled HPG with 0.5 wt % unlabeled HPG added were performed. The fourth series of experiments were time-resolved fluorescence anisotropy measurements on the labeled HPG as a function of concentration in water. Finally, several measurements were undertaken on HPG which was cross-linked using borate ions. The gels were produced at high HPG concentrations where the labeled HPG was added as a tracer at a concentration optimized for the fluorescence measurements.

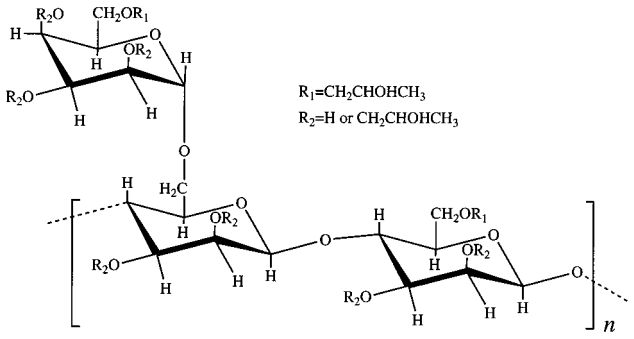

Figure 1. Structure of HPG.

Experimental Details

Solution Preparation. HPG, the derivatized form of Guar gum, was obtained from Rhodia, North American Chemicals, Cranbury, NJ (Jaguar HP-8000, guar hydroxypropyl ether). The substitution of the hydroxyl groups on the sugar rings with hydroxypropyl groups is achieved by reaction between guar and propylene oxide under alkaline conditions.[2] The HPG studied here is such that a small percentage (molar substitution of 0.3−1.6)[1,22] of the hydroxyl groups on the sugar rings are substituted with hydroxypropyl groups (Figure 1). This conversion of guar to HPG results in the product having much less insoluble residue present than the parent guar as well as having better temperature stability in solution. The chain backbone units of HPG are mannose rings, and the side unit is a galactose sugar. The ratio of mannose to galactose units is reported to be between 1.6:1 and 1.8:1,[23] with the spacing of the galactose side groups being random rather than ordered.[24] The weight-average molecular weight of the HPG used was of order 3 million.[25]

A sample of fluorescein-labeled HPG was also provided by Rhodia, Complex Fluids Laboratory. The fluorescent labeling was achieved through a process of partial dissolution of natural guar in DMSO and pyridine, followed by the addition of fluorescein isothiocyanate (FITC) and dibutyltin dilaurate (DTDL). FITC is used to label HPG via reaction between its cyanate group and the alcohol groups along the sugar unit in the polysaccharide. Steric hindrance, however, may restrict the site of attachment to a limited number of alcohol groups. 2-Propanol (IPA) is introduced to the mixture to induce precipitation of the guar and dissolution of the unreacted impurities. IPA is continuously used throughout the procedure to further purify the modified guar product. Approximately 3% of the sugar units along the polysaccharide are labeled with the fluorophore.

Viscosity and Rheological Measurements. Viscosities of the glycerol/water systems were measured using an automated capillary viscometer (Schott AVS 350) regulated to a temperature of 20 °C. Rheological measurements were carried out on a Carry-Med CSL^{2}100 controlled stress rheometer using the cone/plate geometry with a 6 cm cone with an angle of 1′59″ and a truncation of 52 μm.

Absorption and Fluorescence Measurements. Absorption spectra were recorded on a Cary 50 Bio absorption spectrometer. Fluorescence measurements were carried out on both the fluorescently labeled HPG and solutions of unlabeled HPG to which free fluorescein was added. Glycerol−water mixtures ranging from 0 to 100 wt % glycerol (BDH AnalaR) were also used. Water was purified using a Milli-Q system. Glycerol and Milli-Q water were weighed out accordingly, and solutions were mixed well and allowed to stand overnight. Prior to any fluorescence measurements, fluorescein was dissolved in each of these solutions, keeping the absorption at 450 nm below 0.1 to avoid any complications associated with aggregation and inner filtering effects. Bulk solution viscosities were varied through the addition of unlabeled HPG (Rhodia Jaguar HP-8000) to solutions of either fluorescein-labeled HPG or free fluorescein in water/glycerol solutions. Solutions were stirred and heated gently to promote dissolution of HPG in the glycerol/water medium.

Steady-state fluorescence polarization measurements were carried out on either an Hitachi 4500 or a Varian Eclipse fluorimeter with polarization accessory (excitation and emission band-pass settings were both 5 nm, $\lambda_{exc} = 450$ nm and $\lambda_{em} = 500$ nm). Time-resolved fluorescence polarization measurements were carried out using the time-correlated single photon counting method,[26] employing as the excitation source the frequency-doubled output of a mode-locked titanium: sapphire laser (Coherent Mira 900F) ($\lambda_{exc} = 436$ nm, $\lambda_{em} = 507$ nm), pumped by a 12.5 W Ar^+ laser (Coherent Innova 400). This system provided 872 nm pulses of approximately 90 fs duration at 76 MHz. The repetition rate of these pulses was reduced to 4 MHz with a homemade single pass pulse picker based on a TeO_2 Bragg cell (Gooch and Housego) driven by a CAMAC CD5000 electronics unit. The detection electronics were as described elsewhere.[27] Briefly, the fluorescence was collected by an *f*1 quartz lens (Melles Griot), spectrally selected using a monochromator (Jobin Yvon, H20) and detected with a microchannel plate photomultiplier (Hamamatsu R1564U-01). Time-resolved fluorescence anisotropy measurements were carried out by collecting decays with the emission polarization analyzer set parallel and then perpendicular to the direction of the (vertical) polarization of the excitation light. The emission polarization analyzer was switched between the parallel and perpendicular positions for preset periods (usually 30 s dwell times), and the two decays were collected in separate channels of a multichannel analyzer (Tracor Northern ECON II) over total collection periods of approximately an hour in order to enhance the signal-to-noise ratio of the anisotropy function.

The time-resolved fluorescence anisotropy function, $r(t)$, is calculated using eq 1

$$r(t) = \frac{I_{||}(t) - GI_{\perp}(t)}{I_{||}(t) + 2GI_{\perp}(t)} \quad (1)$$

in which $I_{||}(t)$ and $I_{\perp}(t)$ are the individual decays collected with the polarization analyzer set parallel and perpendicular to the vertically polarized excitation light. The "*G*" factor is included to account for any polarization bias of the detection system. The influence of this term was minimized by arranging the polarization analyzer to be the first element in the detection system and using a polarization scrambler immediately prior to the emission monochromator. The steady-state fluorescence anisotropy function, *R*, was calculated in the same way at several wavelengths around the emission maximum and averaged.

The analysis of time-resolved fluorescence anisotropy data can become complex for even relatively simple systems. Various analysis methods, appropriate for specific analysis functions, have been discussed in the literature,[28,29] but because of the complexities involved with analyzing data from polymer systems in general, comprehensive analysis using particular analysis functions was not attempted here. In this work, data analyses were conducted in a number of ways depending on the relevant time scale. For the rapidly depolarizing systems (up to ∼30 wt %), the method of autoreconvolution[28] was employed, whereas for the longer time scale processes, the raw anisotropy decay was fitted without reconvolution using single- or double-exponential decay functions. A double-exponential decay function was required in the case of the fluorescein-bound HPG over the range of HPG concentrations used.

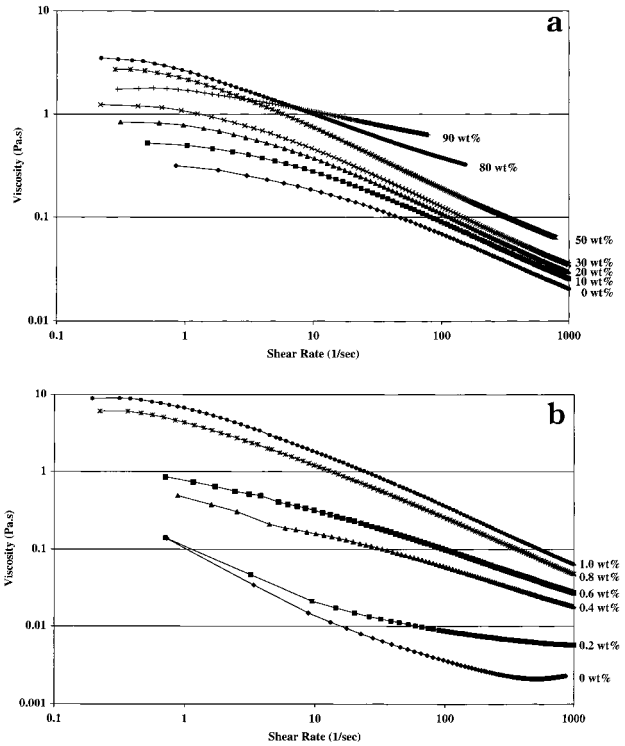

Figure 2. Viscosity vs shear rate curves for (a) HPG (0.5 wt %) in glycerol/water mixtures as a function of glycerol wt % and (b) HPG in water as a function of polymer concentration.

Results and Discussion

Rheometry Measurements. As mentioned in the Introduction, the bulk viscosities of guar and its derivatives are able to be varied over several orders of magnitude as a function of modest polymer concentrations. This is illustrated in Figure 2, which shows the viscosity vs shear rate behavior of HPG (0.5 wt %) in glycerol/water mixtures and HPG over the 0.1−1 wt % concentration range in water. Equilibrium flow measurements enable the determination of a low shear Newtonian plateau. Figure 2b shows that the bulk viscosity of HPG in water reaches values significantly exceeding that of the very viscous glycerol/water mixtures, over the modest range of HPG concentrations used. Figure 2a also shows a low shear plateau for the 90 wt % glycerol curve, whose low shear viscosity is lower than that of the 50 and 80 wt % solutions, indicative of a reduction in the coil size in solution at these high glycerol concentrations. The critical overlap concentration (c^*) for HPG in water has been reported previously from data of this type to be ∼0.21 wt %.[25]

Steady-State Fluorescence Measurements. 1. Unbound Fluorescein Systems. Steady-state and time-resolved fluorescence anisotropy measurements have been conducted on unbound fluorescein in solutions over a range of glycerol/water concentrations (Newtonian solvent viscosity). The steady-state anisotropy values, as plotted in Figure 3, show an interesting trend. There is an approximately linear dependence of

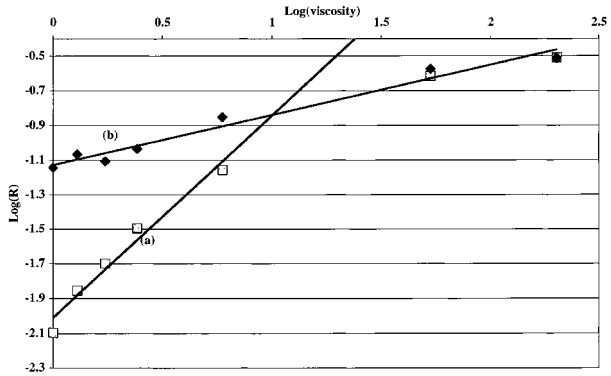

Figure 3. Steady-state fluorescence anisotropy values, *R*, vs bulk viscosity (a) free fluorescein (large squares) and (b) bound fluorescein-HPG (small diamonds) both in the presence of 0.5 wt % HPG, with the viscosity varied through the glycerol/water content. The linear fit for (a) is through the lower five data points only.

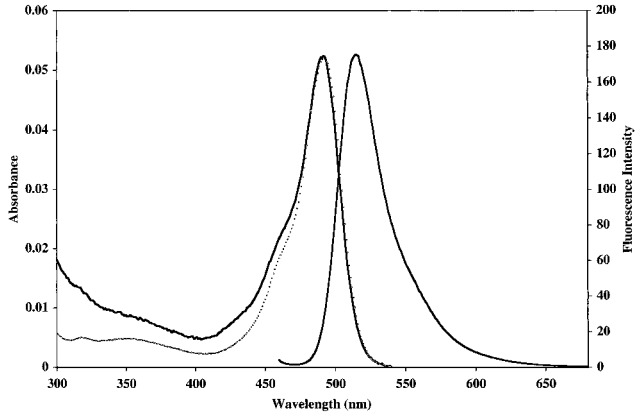

Figure 4. Absorption, fluorescence excitation (dots), and emission spectra of FITC bound to HPG.

anisotropy on viscosity at low viscosities while at higher viscosities the anisotropy values asymptote toward ~0.32, which is close to the limiting (intrinsic) anisotropy of fluorescein.[30] The intrinsic anisotropy is related to the angle between the absorption and emission transition dipoles of the fluorophore. This asymptotic behavior reflects the time scales over which the fluorescence lifetime of fluorescein is appropriate to report on rotational behavior; at high viscosities, the probe rotation is slowed beyond the useful range of this probe and thus limits to the intrinsic anisotropy of the probe.

The addition of unlabeled HPG (0.5 wt %) to the solutions of free fluorescein in glycerol/water made no measurable change to the steady-state fluorescence anisotropy values, despite this HPG concentration being well above *c**. This indicates that the free fluorescein behaves as if it were in the pure glycerol/water mixtures and that the rotation of the fluorescein is not hindered by the presence of the polymer network assumed to be operative at this polymer concentration. These results also indicate that there is no binding or affinity of the fluorophore for the HPG in solution and that the solution is essentially homogeneous in glycerol/water. This is despite the observation that the HPG coil reduces in size in the 90 wt % glycerol solution.

2. Bound Fluorescein Systems. The absorption and fluorescence spectra of the fluorescein-labeled HPG are shown in Figure 4, from which it is seen that the spectra are not significantly different from fluorescein in water.[31]

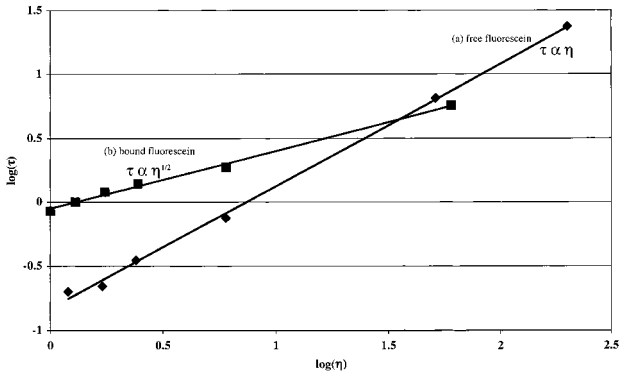

Figure 5. Rotational correlation times vs bulk viscosity (a) free fluorescein in the presence of 0.5 wt % HPG (diamonds) and (b) bound fluorescein-HPG (squares) as a function of viscosity varied through glycerol/water content.

The steady-state fluorescence anisotropy values obtained from the bound fluorescein with 0.5 wt % unlabeled HPG added as a function of glycerol/water concentrations can be compared with the corresponding values obtained from the free fluorescein system (Figure 3). The higher anisotropy intercept of the bound form compared to the free fluorescein reflects the restricted motion of the bound probe. It is seen that there is a vastly different dependence of the steady-state fluorescence anisotropy on viscosity for the two systems. The anisotropy values at high viscosity are essentially identical, while there is a linear dependence on the logarithmic scale of the anisotropy with viscosity for the bound probe. This dependence leads to a power law behavior of the form $R \propto \eta^{\alpha}$; in this case α is found to have a value of ~0.3. The implications of this finding are discussed below.

For the labeled HPG in water at a range of unlabeled HPG concentrations, the steady-state anisotropy is insensitive to the polymer concentration at concentrations up to ~1 wt %. Measurement at an HPG concentration of 10 wt % showed a small increase in the steady-state anisotropy ($R \sim 0.12$) relative to the lower concentrations. This reflects the first noticeable evidence of interactions between the polymer chains reported by the fluorescent probe. The onset of the interaction between polymer chains as sensed by the fluorescent probe occurs at concentrations significantly above *c**.

Time-Resolved Fluorescence Measurements. 1. Unbound Fluorescein Systems. The fluorescence decays of unbound fluorescein with 0.5 wt % unlabeled HPG added collected at the magic angle (54.7°), and the fluorescence anisotropy decays from these solutions are essentially exponential over the range of glycerol contents measured. The rotational correlation times derived from these anisotropy decays are plotted in Figure 5 as a function of solvent viscosity. The fluorescence decay times, rotational correlation times, and initial anisotropy values agree well with those reported by Lakowicz et al.[30]

The rotational correlation times, τ_{or}, determined from the time-resolved fluorescence anisotropy measurements of free fluorescein in a range of water/glycerol mixtures show a simple linear relationship with solvent viscosity (Figure 5). An empirical form of the relationship between the free rotor time (i.e., in the absence of solvent), τ_0, and the viscosity, η, is[32]

$$\tau_{or} = c\eta + \tau_0 \qquad (2)$$

In the case of fluorescein, the limiting rotor time, τ_0, would be expected to be negligibly small as has been reported for molecules such as DODCI[32] and is neglected in the following discussion for simplicity. The factor c is determined by the size and shape of the molecule and the hydrodynamic boundary conditions. For the case of a simple spherical rotor with stick boundary conditions, the Debye−Stokes−Einstein theory can be implemented, and c is given by V/kT. Under such conditions, the free probe rotational diffusion constant can be described by

$$D = \frac{kT}{6V\eta} = \frac{kT}{8\pi\eta r^3} \tag{3}$$

where k is Boltzmann's constant, T the absolute temperature, η the solvent viscosity, r the rotational hydrodynamic radius of the spherical diffusing object, and V the hydrodynamic volume.

The radius of the fluorescein calculated from the rotational diffusion coefficient assuming spherical geometry ($\tau_{or} = 1/6D$) (0.5 nm) is approximately equal to the radius of the fluorescein in its planar orientation. The free rotation in solution will be an average of rotation about the different axes of the molecule. The fluorescein is relatively planar, and the thickness of the disk would be expected to be of order several angstroms. The data indicate that the dominant rotational modes occur with the free fluorescein rotating as a disk in the plane resembling a flying saucer.

The addition of unlabeled HPG (again to 0.5 wt %) to the unbound fluorescein/glycerol/water solutions does not change the fluorescence decay or fluorescence anisotropy characteristics to any measurable degree. This is consistent with the steady-state findings reported above and confirms the lack of association of the free probe to the polymer and that preferential solvation of the unbound fluorescein is not occurring.

2. Bound Fluorescein in Glycerol/Water Mixtures. The fluorescence decay of the fluorescein-labeled HPG is, unlike the unbound case, nonexponential. Nonexponential decay behavior is commonly observed for probes attached to polymers and is often attributed to a variation in the local environments of the range of potential sites of the attached probe molecules on the polymer backbone (Figure 1). This complicates subsequent interpretation of the time-resolved fluorescence anisotropy measurements, and for this reason a simple sum-of-exponentials analysis function was used in the following data interpretation.

The fluorescence anisotropy from the bound fluorescein glycerol/water systems decays in a nonexponential manner, with a double-exponential decay (or a single-exponential component with a baseline term) being adequate to describe the decay to a first approximation. Given the baseline noise inherent in fluorescence anisotropy measurements and the short fluorescence lifetime of the FITC probe used (relative to the time scales involved in the second term), the origin and nature of this term have not been conclusively determined. However, its inclusion in the analysis was necessary to provide accurate determination of the rapid component which was the dominant contributor and of most relevance in the present context. The data shown in Figure 6 are derived from a double-exponential decay analysis. The anisotropy decays consist of a rapid decay component (>80%) which varies with solvent viscosity

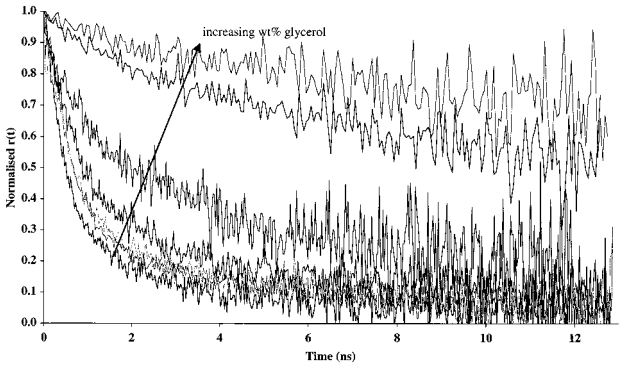

Figure 6. Fluorescence anisotropy decays of bound fluorescein-HPG in a range of glycerol/water mixtures (0.5 wt % unlabeled HPG added).

as expected and a minor (<20%) contribution by a long (>10 ns) component. The relative magnitudes of these components were invariant with glycerol concentration. The reduced signal-to-noise at longer times in the high-viscosity regime is related to the relatively short fluorescence lifetime of the fluorescence probe used. In the results reported below, only the shorter component is considered where plotting this term as a function of the bulk solution viscosity results in several interesting findings. It should be noted that the simple interpretation used yields similar trends to the steady-state anisotropy data, vindicating the straightforward approach used.

Figure 5 shows that in the labeled HPG in glycerol/water mixtures the probe is sensitive to the solvent viscosity in a manner not predicted by eq 2, but rather is described by eq 4

$$\tau_{or} = c\eta^{\alpha} \tag{4}$$

with $\alpha \sim 0.5$ (again neglecting any limiting rotor time, τ_0, term). The value of $\log(\tau_{or})$ as $\log(\eta)$ tends to zero is related to the effective volume taken up (swept out) by the rotating fluorophore through the factor c. This volume would be expected to differ between the free and bound forms of the fluorescein due to the reduced degrees of freedom of the bound form.

The rotational motion of the bound fluorescein probe is restricted by the attachment to the polymer backbone by the central (linkage) axis. At low viscosities, the magnitudes of the rotational correlation times corresponding to the free and bound forms of the fluorescein (Figure 5) differ. The larger rotational correlation time infers a larger rotating entity, given that the slip boundary conditions are the same for both probes in a given solvent. The rotational size interpreted for the bound form from the rotational correlation time using eq 3 (0.94 nm in water) is greater than the size of the calculated planar radius of fluorescein[33] (0.8 nm), in contrast to the value interpreted for the free fluorescein (0.5 nm).

The key finding illustrated in Figure 5 is the nonlinear ($\tau_r \sim \eta^{\alpha}$) dependence of the rotational relaxation time of the probe on the solvent viscosity, where $\alpha \sim {}^1/_2$. This is in contrast to the observed behavior of the unbound fluorescein where $\alpha \sim 1$. The value of α from the time-resolved measurements, while somewhat different in magnitude to that concluded from the steady-state measurements ($\alpha \sim 0.3$), is consistent with the steady-state data (Figure 3) in showing a nonlinear viscosity dependence. A similar power law dependence

of the rotational correlation time with viscosity has been reported for other systems where α values of 0.75 and 0.41 have been found.[9,19,34]

The power law dependence of the rotational correlation time on viscosity has been explained in other studies using a modified Kramers' theory.[35] Kramers' theory provides a commonly used framework for the quantitative interpretation of molecular dynamics in solution. Kramers' equation was originally derived to explain isomerization reactions and shows a linear dependence of the rotational correlation time with viscosity. The observed nonlinear dependence of τ on η has led to an empirical modification of Kramers' equation in order to interpret the results in terms of an activation energy for the rotation of the fluorophore.[35] This empirical modification is not considered to be entirely applicable to the system under investigation here and has therefore not been applied to the interpretation of the data reported herein. The isomerization type approach is more appropriate to the mid-chain-bound chromophore which must rotate through an isomerization type reaction rather than the pendant chromophore used in this study. The modification of Kramers' theory is purely empirical and does not give further insight into the physics associated with the α values obtained. It should also be noted that Ediger also concludes that Kramers' theory is not appropriate for describing the local chain dynamics of many synthetic polymers.[34]

Both the α values and hydrodynamic sizes inferred from the data for the bound fluorescein in this study are presumably due to the reduced rotational degrees of freedom associated with the attached chromophore. The unbound fluorophore rotates randomly in three dimensions while the pendant fluorophore must rotate around its central axis parallel to the covalent bond linking the probe to the polymer backbone. It is of interest that the steady-state data for the free fluorophore show a linear dependence on the viscosity at low concentrations and plateaus to the limiting inherent anisotropy for the fluorescein at high glycerol concentrations. As such, the power law dependence must derive from the intrinsic anisotropy of the chromophore, the rotational degrees of freedom, the solvent viscosity, and a component due to the bulk viscosity from chain−chain interactions. Park and Waldeck[36] have considered the isomerization dynamics of stilbene and conclude that α values less than unity arise from the reduced dimensionality of the diffusion.

3. Bound Fluorescein in Water as a Function of Polymer Concentration. The measured viscosities of the aqueous solutions over a range of HPG concentrations in water vs shear rate are shown in Figure 2. As is readily seen, the polymer solution viscosities are several orders of magnitude greater than that of the pure solvent, even at relatively low HPG concentrations. The anisotropy decays of the bound fluorescein at the different HPG concentrations are shown in Figure 7. The decrease in signal-to-noise at the highest HPG concentration shown is due to increased scattering from the solution. There is little difference observed in the fluorescence anisotropy decay curves up to 1 wt % in solution. The 10 wt % solution shows that a long rotational correlation time component is present with the relative contributions to the total anisotropy decay of the rapid and slow processes being approximately equal. The probe molecule is therefore sensing the

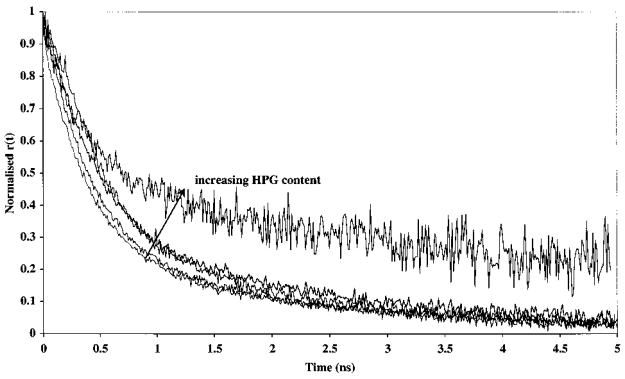

Figure 7. Time-resolved fluorescence anisotropy decays for labeled HPG as a function of HPG concentration in water (concentrations of added HPG are 0.2, 0.4, 0.6, 0.8, and 10 wt %).

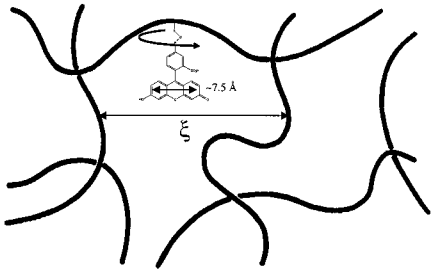

Figure 8. Schematic of mesh size and attachment of fluorophore.

presence of the neighboring molecules to a measurable degree at this concentration. It should be noted that while the viscosity data are not shown for the 10 wt % solution, this solution is effectively a free-standing solid. The mesh size or correlation length, ξ, is defined as a function of the polymer fraction (Φ, defined as the fraction of sites occupied by monomers), by $\xi \propto (\Phi/\Phi^*)^{3/4}$ where Φ* is the critical polymer fraction which is related to the critical concentration by $\Phi^* = c^* a^3$, where a^3 is the volume of the unit cell in a cubic lattice.[3] The value of ξ for the polymer solution at 10 wt % concentration is calculated to be of order 5 nm.[3] This correlation length is still considerably larger than the physical size of the probe molecule (∼0.8 nm as discussed above) and shown in Figure 8. The interaction between the HPG molecules which gives rise to the solution viscosity should be strong at concentrations of 10 wt %, which is significantly higher than the critical overlap concentration of 0.2 wt %.[25]

To effect additional interaction between the polymer chains, cross-linking of the HPG using borate ions was undertaken.[25] This was done with tracer amounts of the fluorescein-labeled HPG incorporated into the gel. The magic angle fluorescence decays of the gelled HPG systems are (at least) double exponential with decay times of ∼0.75 and ∼4.2 ns. No attempt to assign these decay terms to particular species has been made (although the ∼4 ns term is very close to that of fluorescein). The magic angle decays of the ungelled systems containing labeled guar show very similar decay times. The fluorescence anisotropy data for the HPG at three concentrations with the same ratio of borate ions as the cross-linker (maintained at pH 12) are shown in Figure 9. There are observed two anisotropy decay times with the rapid component being faster than that observed for the bound fluorescein in solution and with the longer component being slower than that

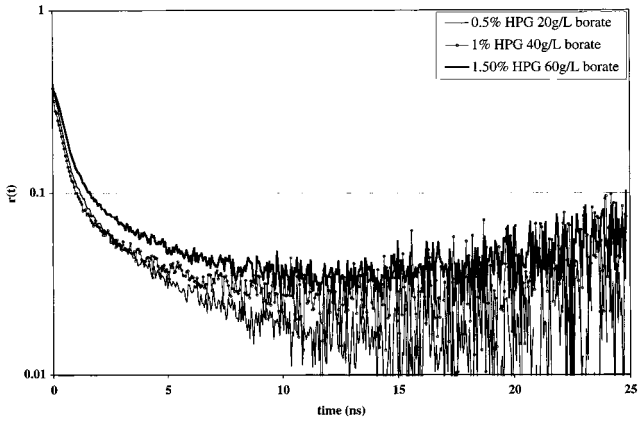

Figure 9. Time-resolved fluorescence anisotropy profiles of HPG cross-linked by use of borate ions.

observed in solutions of concentrated HPG. The anisotropy decay curves show minima and then appear to increase after long times. This behavior has been observed previously for heterogeneous systems where dye molecules were attached to colloidal particles[29] and other polymer systems;[37] however, the reasons for the rise in anisotropy at longer times in the present system are not fully understood. The gelation of the HPG causes a separation of the rotational lifetimes into both a very rapid and a long component. This results from the probe molecules experiencing two environments. Some of the probe molecules will experience a region close to cross-linking sites resulting in slowed rotational motion while the others will be located far from the cross-link points and experience only the free solvent.

Conclusions

The free fluorescein in glycerol/water mixtures senses the solution viscosity in a manner predicted by the Stokes−Einstein−Smoluchowski equation. The rotational motion of the free fluorescein is found to be unaffected by the presence of the HPG polymer at concentrations significantly exceeding the critical overlap concentration. In contrast, the bound fluorescein shows a $\tau \sim \eta^{1/2}$ dependence in the glycerol/water solutions due to restricted motion of the probe. The rotational correlation time of the bound probe is relatively insensitive to the concentration of the polymer in solution up to ~1 wt %. A somewhat surprising result is that the onset of measurable polymer chain interaction (as sensed by the rotational motion of the probe) is only observed to occur at concentrations far in excess of c^*. At 10 wt % concentration of HPG in solution, the probe senses the presence of the other polymer chains, and a slowing of the rotational diffusion of the probe molecule is observed.

Gelling the HPG using borate ions as the cross-linking agent yields a rapid and a slow rotational correlation time. The observed anisotropy decay curves are consistent with the system becoming heterogeneous at a molecular level under these conditions.

Acknowledgment. We gratefully acknowledge the provision of the fluorescein-labeled HPG by Dr. Jeannie Chang of Rhodia, Complex Fluids Laboratory, Cranbury USA. The use of the laser equipment was graciously provided by Prof. Ken Ghiggino. The assistance of Ms Briony Ruse in the cross-linking measurements is also acknowledged.

References and Notes

(1) *Guar, Locust Bean, Tara, and Fenugreek Gums*, 3rd ed.; Maier, H., Anderson, M., Karl, C., Magnuson, K., Eds.; Academic Press: San Diego, 1993.
(2) Lapasin, R.; Pricl, S. *Rheology of Industrial Polysaccharides: Theory and Applications*; Blackie Academic & Professional: London, 1995.
(3) DeGennes, P.-G. *Scaling Concepts in Polymer Physics*; Cornell University Press: London, 1979.
(4) Morawetz, H. *Polym. Prepr.* **1986**, *27*, 316−317.
(5) Daoud, M.; Cotton, J. P.; Farnoux, B.; Jannink, G.; Sarma, G.; Benoit, H.; Duplessis, J. P.; Picot, C.; DeGennes, P.-G. *Macromolecules* **1975**, *8*, 804−818.
(6) Oster, G.; Nishijima, Y. *Fortschr. Hochpolym.-Forsch* **1964**, *3*, 313−331.
(7) Biddle, D.; Pardhan, S. *Ark. Kemi* **1970**, *32*, 43−53.
(8) Hu, Y.; Horie, K.; Ushiki, H. *Macromolecules* **1992**, *25*, 6040−6044.
(9) Adolf, D. B.; Ediger, M. D.; Kitano, T.; Ito, K. *Macromolecules* **1992**, *25*, 867−872.
(10) Johnson, B. S.; Ediger, M. D.; Kitano, T.; Ito, K. *Macromolecules* **1992**, *25*, 873−879.
(11) Soutar, I.; Swanson, L. *Macromolecules* **1994**, *27*, 4304−4311.
(12) Jarry, J. P.; Erman, B.; Monnerie, L. *Macromolecules* **1986**, *19*, 2750−2755.
(13) Monnerie, L. In *Photophysics of Synthetic Polymers*; Phillips, D., Roberts, A., Eds.; Science Reviews: Northwood, 1982; pp 70−81.
(14) Valeur, B.; Monnerie, L. *J. Polym. Sci.* **1976**, *14*, 11−27.
(15) Viovy, J. L.; Monnerie, L. *Polymer* **1986**, *27*, 181−184.
(16) Kasparyan-Tardiveau, N.; Valeur, B.; Monnerie, L. *Polymer* **1983**, *24*, 205−208.
(17) Bur, A. J.; Lowry, R. E.; Roth, S. C.; Thomas, C. L.; Wang, F. W. *Macromolecules* **1991**, *24*, 3715−3717.
(18) Bur, A. J.; Lowry, R. E.; Roth, S. C.; Thomas, C. L.; Wang, F. W. *Macromolecules* **1992**, *25*, 3503−3510.
(19) Ono, K.; Okada, Y.; Yokotsuka, S.; Sasaki, T.; Yamamoto, M. *Macromolecules* **1994**, *27*, 6482−6486.
(20) Clements, J. H.; Webber, S. E. *J. Phys. Chem. A* **1999**, *103*, 2513−2523.
(21) Ushiki, H.; Ozu, M. *Eur. Polym. J.* **1986**, *22*, 835−839.
(22) Prud'Homme, R. K.; Constein, V.; Knoll, S. In *SPE 18210, 63rd Annual Technical Conference and Exhibition*; Houston, TX, 1987.
(23) Gulbis, J. *Fracturing Fluid Chemistry*; Schlumberger Educational Services: Houston, TX, 1987; Chapter 3.
(24) McCleary, B. V.; Clark, A. H.; Dea, I. C. M.; Rees, D. A. *Carbohydr. Res.* **1985**, *139*, 237−260.
(25) Power, D. J. PhD Thesis, University of Melbourne, 1997.
(26) O'Connor, D. V.; Phillips, D. *Time-Correlated Single Photon Counting*; Academic Press: London, 1984.
(27) Smith, T. A.; Haines, D. J.; Ghiggino, K. P. *J. Fluoresc.* **2000**, *10*, 365−373.
(28) Rumbles, G.; Smith, T. A.; Brown, A. J.; Carey, M.; Soutar, I. *J. Fluoresc.* **1997**, *7*, 217−229.
(29) Smith, T. A.; Irwanto, M.; Haines, D. J.; Ghiggino, K. P.; Millar, D. P. *Colloid Polym. Sci.* **1998**, *276*, 1032−1037.
(30) Lakowicz, J. R.; Cherek, H.; Maliwal, B. P. *Biochemistry* **1985**, *24*, 376−383.
(31) Haugland, R. P. *Handbook of Fluorescent Probes and Research Chemicals*, 7th ed.; Molecular Probes: Oregon, 1999.
(32) Fleming, G. R. *Chemical Applications of Ultrafast Spectroscopy*; Oxford University Press: New York, 1986.
(33) "Chem3D", Cambridge Scientific Computing, Inc., 1993.
(34) Glowinkowski, S.; Gisser, D. J.; Ediger, M. D. *Macromolecules* **1990**, *23*, 3520−3530.
(35) Courtney, S. H.; Fleming, G. R. *J. Chem. Phys.* **1985**, *83*, 215−222.
(36) Park, N. S.; Waldeck, D. H. *J. Chem. Phys.* **1989**, *91*, 943−952.
(37) Chee, C. K.; Ghiggino, K. P.; Smith, T. A.; Rimmer, S.; Soutar, I.; Swanson, L. *Polymer* **2001**, *42*, 2235−2240.

MA010954P